Relevance of Partially Structured States in the Non-Classical Secretion of Acidic Fibroblast Growth Factor†

Dakshinamurthy Rajalingam,‡ Irene Graziani,§ Igor Prudovsky,§ Chin Yu,*,‡,|| and Thallapuranam Krishnaswamy S. Kumar*,‡

Department of Chemistry and Biochemistry, University of Arkansas, Fayetteville, Arkansas 72701, Center for Molecular Medicine, Maine Medical Center Research Institute, Scarborough, Maine 04074, and Department of Chemistry, National Tsing Hua University, Hsinchu 30043, Taiwan

Received February 6, 2007; Revised Manuscript Received June 5, 2007

ABSTRACT: Acidic fibroblast growth factor (aFGF) is a signal peptide-less protein that is secreted into the extracellular compartment as part of a multiprotein release complex, consisting of aFGF, S100A13 (a calcium binding protein), and a 40 kDa (p40) form of synaptotagmin (Syt1), a protein that participates in the docking of a variety of secretory vesicles. p40 Syt1, and specifically its C2A domain, is believed to play a major role in the non-classical secretion of the aFGF release complex mediated by the interaction of aFGF and p40 Syt1with the phospholipids of the cell membrane inner leaflet. In the present study, we investigate the structural characteristics of aFGF and the C2A domain of p40 Syt1 under acidic conditions, using a variety of biophysical techniques including multidimensional NMR spectroscopy. Urea-induced equilibrium unfolding (at pH 3.4) of both aFGF and the C2A domain are non-cooperative and proceed with the accumulation of stable intermediate states. 1-Anilino-8-napthalene sulfonate (ANS) binding and size-exclusion chromatography results suggest that both aFGF and the C2A domain exist as partially structured states under acidic conditions (pH 3.4). Limited trypsin digestion analysis and ^{1}H-^{15}N chemical shift perturbation data reveal that the flexibility of certain portions of the protein backbone is increased in the partially structured state(s) of aFGF. The residues that are perturbed in the partially structured state(s) in aFGF are mostly located at the N- and C-terminal ends of the protein. In marked contrast, most of the interactions stabilizing the native secondary structure are preserved in the partially structured state of the C2A domain. Isothermal titration calorimetry data indicate that the binding affinity between aFGF and the C2A domain is significantly enhanced at pH 3.4. In addition, both aFGF and the C2A domain exhibit much higher lipid binding affinity in their partially structured states. The translocation of the multiprotein FGF release complex across the membrane appears to be facilitated by the formation of partially structured states of aFGF and the C2A domain of p40 Syt1.

Fibroblast growth factors (FGF) are ∼17 kDa β-sheet proteins that play crucial roles in the regulation of key cellular processes, such as angiogenesis, morphogenesis, differentiation, and tumor growth (*1*−*5*). The biological functions of FGFs are mediated by a family of transmembrane tyrosine kinase receptors, FGFRs (*6*−*8*). Therefore, FGFs are required to be secreted into the extracellular compartment for them to bind to their cell surface receptors and exhibit their mitogenic activity. Paradoxically, both acidic and basic FGFs, two prototypic members of the FGF family, lack the conventional amino-terminal signal sequence required for the secretion of proteins through the classical endoplasmic reticulum (ER)−Golgi secretory pathway (*9*−*11*). Previously, Maciag and co-workers showed that under cellular stress, aFGF[1] is exported through a non-classical release pathway involving the formation of a specific copper (Cu^{2+})-dependent multiprotein complex (*12*−*14*). The protein constituents of this complex include the aFGF homodimer, the small calcium (Ca^{2+}) binding protein, S100A13 (*15*−*18*), and the 40 kDa (p40) cytosolic form of synaptotagmin 1 (Syt1), a transmembrane docking protein that participates in exocytosis (*19*−*21*). The exact mechanism of the formation of the multiprotein FGF complex and its release into the extracellular compartment is still not clear.

Prudovsky et al., studying the spatio-temporal parameters of the stress-induced aFGF release, showed that the proteins involved in the multiprotein aFGF release complex are co-

† This study was supported by research grants from the National Institutes of Health (NIH NCRR COBRE Grant, P20RR15569), Department of Energy (DE-FG02-O1ER15161), and the Arkansas Bioscience Institute to T.K.S.K. C.Y. was supported by the National Science Council, Taiwan (NSC 94-2320-B007-005 and NSC-94-2113-M007-036). I.P. and I.G. were supported by NIH Grants HL32348, HL35627, and RR15555 (project 4).

* To whom correspondence should be addressed. Phone: 479-575-5646. Fax: 479-575-4049. E-mail: sthalla@uark.edu (T.K.S.K.). Phone: 886-35-711082. Fax: 886-35-721524. E-mail: cyu@mx.nthu.edu.tw (C.Y.).

‡ University of Arkansas.

§ Maine Medical Center Research Institute.

|| National Tsing Hua University.

[1] Abbreviations: ITC, isothermal lcalorimetry; ANS, 1-anilino-8-napthalene-sulfonate; CD, circular dichroism; aFGF, acidic fibroblast growth factor; SUVs, small unilamellar vesicles; pS, L-α-phosphatidylserine; HSQC, heteronuclear single quantum coherence; NMR, nuclear magnetic resonance.

10.1021/bi7002586 CCC: $37.00
Published on Web 07/18/2007

localized near the inner surface of the plasma membrane (*22*). It is believed that the membrane-binding properties of aFGF and the C2A domain of p40 Syt1 are important for the translocation of the multiprotein aFGF release complex across the membrane bilayer (*21*−*24*). There have been several attempts to understand the general mechanism of the translocation of aFGF across the plasma membrane. Wiedlocha et al., using a fusion protein of aFGF and diphtheria toxin A-fragment disulfide-linked to toxin B-fragment, demonstrated that partial unfolding of aFGF is crucial for its secretion into the extracellular compartment of the cell (*25*). Later, Wesche et al, using disulphide-bonded aFGF mutants, found that the extensive unfolding was not required for membrane translocation of aFGF mediated by FGF receptors (*26*). Several studies from the Middaugh group revealed that aFGF at neutral pH, ambient temperature, and low ionic strength exists in a partially structured state that is capable of strong interaction with membrane vesicles (*27*−*30*). Recently, Fan et al., using the empirical phase diagram approach, showed that heparin protects aFGF against acid-induced unfolding (*31*). In addition, Sanz and Gallego showed that aFGF exhibits high lipid binding affinity at acidic pH (*32*). We have recently demonstrated that the mutations of specific lysine clusters in aFGF and p40 Syt1 result in a significant decrease of their ability to destabilize liposomes composed of acidic phospholipids and a dramatic inhibition of their non-classical release from the cells (*33*). Bychkova et al., investigating the structure of cytochrome *c* under acid conditions, suggested that the negative membrane potential creates an acidic microenvironment that in-turn causes a denaturation effect on proteins, leading to their partial unfolding (*34*). The partially structured states, generated at the membrane surface, are believed to be highly competent to traverse across membrane bilayers (*34*, *35*). In this context, in our quest to understand the possible effects of the acidic microenvironment (such as at the membrane surface) on the multiprotein FGF release complex, we embarked on a study to compare the structural characteristics of aFGF and the C2A of p40 Syt1 domain under acidic and neutral conditions. C2A domain of p40 Syt1 binds to cell membranes, and its Ca^{2+}-binding loops or "prongs" the penetrate phospholipid bilayers (*21*).

In this study, we investigate the pH-induced unfolding of aFGF and the C2A domain of p40 Syt1 using a variety of biophysical techniques including multidimensional NMR spectroscopy. The results obtained reveal that both proteins exist as partially structured states under acidic conditions. The binding affinity between the C2A domain and aFGF is also observed to increase significantly under acid conditions (at pH 3.4). In addition, the partially structured states of both aFGF and the C2A domain interact strongly with membrane vesicles. The results of the present study clearly suggest that membrane-binding affinities of the C2A domain and aFGF are important for the membrane translocation of the multiprotein FGF release complex.

MATERIALS AND METHODS

Ingredients for Luria Broth were obtained from AMRESCO. Aprotinin, pepstatin, leupeptin, phenylmethylsulfonyl fluoride, Triton X-100, terbium chloride, and β-mercaptoethanol were obtained from Sigma Co. (St. Louis). Heparin−sepharose and glutathione−sepharose were obtained from Amersham Pharmacia Biotech. Labeled $^{15}NH_4Cl$ and D_2O were purchased from Cambridge Isotope Laboratories. All other chemicals used were of high quality analytical grade. All experiments were performed at 25 °C. Unless specified, all solutions were made in 10 mM sodium phosphate containing 100 mM NaCl.

Expression and Purification of aFGF. Overexpression and purification of aFGF was achieved using methods reported by Arunkumar et al. (*2*).

Expression and Purification of the C2A Domain. cDNA encoding the C2A domain of synaptotagmin I (residues 140 to 267) and p40 Syt1 was kindly provided by Professor Thomas Sudhof. *E. coli* expressing C2A were induced with isopropyl-β-D-thiogalactopyranoside (IPTG) when absorbance (absorbance at 600 nm) reached 0.5−0.6, and the cells were harvested by centrifugation at 6,000 rpm after 4 h of induction. The harvested cells were resuspended, and cell walls were ruptured by sonication. The cell lysate was centrifuged at 16,000 rpm for 20 min. The supernatant was then incubated with glutathione−sepharose. For standard preparations, the resin was extensively washed with PBS until there was no detectable UV absorption in the eluate, and the bound protein was cleaved with thrombin (1 NIH unit/mL) at 25 °C for 8 h. The cleaved protein (C2A) was eluted with PBS buffer. The C2A domain obtained was further purified by gel filtration on a superdex-75 (Pharmacia) column by FPLC using 10 mM sodium phosphate (pH 7.0) containing 100 mM NaCl as the eluent. The homogeneity of the protein was assessed using SDS−PAGE. The authenticity of the sample was further verified by electron-spray mass analysis. The concentration of the protein was estimated on the basis of the extinction coefficient value (ϵ_{280nm} = 12090 M^{-1} cm^{-1}) calculated from the amino acid sequence of the C2A domain (*20*).

Preparation of Isotope-Enriched aFGF and the C2A Domain. Uniform ^{15}N labeling of both aFGF and C2A was achieved using M9 minimal medium containing $^{15}NH_4Cl$. To achieve maximal expression yields, the composition of the M9 medium was modified by the addition of a mixture of vitamins. The expression host strain *Escherichia coli* BL21 (DE3) pLysS is a vitamin B1-deficient host, and hence, the medium was supplemented with thiamine (vitamin B1).

Steady-State Fluorescence Measurements. All fluorescence spectra were collected on a Hitachi F-2500 spectrofluorometer at 2.5 nm resolution, using an excitation wavelength of 280 nm. Fluorescence measurements were made at a protein concentration of 50 μM in 10 mM phosphate buffer containing 100 mM NaCl. The fraction of unfolded species formed at various concentrations of urea was estimated on the basis of the intensity at 350 and 340 nm for the C2A domain. Blank corrections were made in all of the spectra using 10 mM sodium phosphate containing 100 mM NaCl.

ANS Binding Experiments. The 1-anilino-8-naphthalenesulfonate (ANS) binding experiments were performed using a Hitachi F-2500 spectrofluorimeter at 25 °C. Fluorescence spectra were acquired using an excitation wavelength of 390 nm and an emission wavelength of 400−600 nm. All protein samples were prepared in 10 mM phosphate buffer (pH 7.0) containing 100 mM NaCl. Phosphoric acid and NaOH were used to adjust the pH of the solutions. The pH of the solutions was checked repeatedly after the addition of the proteins and ANS to ensure the accuracy of the measured pH (with an

error of about ±0.2 pH units). Final spectra were obtained after correcting for the background fluorescence of ANS.

pH-Induced Denaturation. The pH-induced denaturation experiments were monitored by fluorescence (Hitachi F-2500 spectrofluorometer) and far-UV CD (at 228 nm) spectroscopy (AVIV-215 spectropolarimeter) at 25 °C. Protein samples were prepared in 10 mM sodium phosphate containing 100 mM NaCl. Phosphoric acid (10 mM) was titrated with 1 M NaOH to obtain the required pH. The pH of the solutions were checked repeatedly after the addition of the protein or urea, or both. A maximum variation of ±0.2 pH units was allowed in all buffer preparations. Blank corrections were made in all of the spectra using 10 mM sodium phosphate buffer containing 100 mM NaCl.

Urea-Induced Unfolding. Urea-induced equilibrium unfolding, under various pH conditions, was monitored by far-UV CD (ellipticity changes at 228 nm for aFGF and 218 nm for the C2A domain) and by intrinsic tryptophan fluorescence (at 350 nm for aFGF and, at 340 nm for the C2A domain). For the unfolding experiments, protein samples were dissolved in appropriate concentrations of urea prepared in 10 mM sodium phosphate (at the desired pH) containing 100 mM NaCl. Necessary background corrections were made in all of the spectra.

Equilibrium Unfolding and Data Analysis. Equilibrium unfolding data obtained were converted to plots of F_u, fractions of the protein in the unfolded state, versus denaturant concentration using the following equation:

$$F_u = (X_D - (X_F + m_F[D])/ (X_u + m_U[D]) - (X_U + m_F[D])$$

where, X_D is the value of the spectroscopic property measured at a denaturant concentration ([D]). X_F and X_U represent intercepts, and m_F and m_U are the slopes of the folded and unfolded baselines of the data, respectively, and were obtained from the linear least-square fits of the baselines. The unfolding data were fit to a two-state (folded ↔ unfolded) model, and the free energy of unfolding by the denaturant (G_u) at concentration [D] was related to F_U by transforming the Gibbs−Helmholtz equation. It is assumed that the free energy of unfolding, ΔG_u, has a linear dependence on the concentration of the denaturant ([D]).

$$\Delta G_u = \Delta G(H_2O) + m[D]$$

where, $\Delta G(H_2O)$ and m are the intercept and slope, respectively, in the plot of ΔG_u versus concentration of the denaturant. m is the measure of the cooperativity of the unfolding reaction, and $\Delta G(H_2O)$ is the difference in the free energy between the folded and unfolded states of the protein in the absence of any denaturant.

Circular Dichroism. All CD measurements were made on an AVIV-215 spectropolarimeter using a 1 mm path length quartz cell. Each spectrum was an average of 10 scans. The concentration of the protein used was 50 μM (in 10 mM sodium phosphate containing 100 mM NaCl). The final spectra were obtained after necessary blank corrections with 10 mM sodium phosphate containing 100 mM NaCl.

Size-Exclusion Chromatography. All gel filtration experiments were carried out at various pH (at 25 °C) on a superdex-75 column using an AKTA FPLC device (Amersham Pharmacia Biotech). The column was equilibrated with 2 bed volumes of the buffer (10 mM sodium phosphate containing 100 mM of NaCl) at the appropriate pH (±0.2 units). The flow rate of the eluent was set at 1 mL/min. Protein peaks were detected by their 280 nm absorbance. The concentration of the protein used was about 50 μM.

Proteolytic Digestion Assay. Digestion experiments were carried out by independently incubating aFGF and the C2A domain with trypsin (at 1:1 protein to trypsin molar ratio) in 10 mM phosphate buffer containing 100 mM NaCl. The protease action was stopped by heating the mixture (protein + trypsin) at 90 °C for 10 min. The products of the protease reaction were analyzed by SDS−PAGE analysis. The degree of cleavage was measured by estimating the intensity of the band (on SDS−PAGE) corresponding to aFGF and the C2A domain (remaining after trypsin digestion) using a scanning densitometer. The intensities of the bands corresponding to the untreated aFGF and the C2A domain were considered as a control for 100% protection against trypsin action.

Lipid Preparation. Small unilamellar vesicles (SUV) were prepared by dissolving the solid phospholipid (phosphatidyl serine (pS), purchased from Avanti polar lipid, Inc.) in chloroform, followed by evaporation to dryness under nitrogen. The lipid film was suspended in 10 mM sodium phosphate containing 100 mM NaCl and sonicated in an AQUASONIC-75D12 bath-type sonicator until optical clarity was obtained. The solution was finally centrifuged for 5 min at 14000 rpm in an Eppendorf microfuge before use and stored for a maximum of 6 h in ice.

Isothermal Titration Calorimetry. The binding of aFGF to the C2A domain or the binding of the protein (aFGF/C2A domain) to the lipid vesicles was analyzed by measuring heat change during the titration using VP-ITC titration microcalorimeter (Micro Cal. Inc., Northampton, MA). Experiments were carried out at a constant temperature of 25 °C. The buffer used was 10 mM sodium phosphate containing 100 mM NaCl. The reference cell contained Milli Q water. Upon equilibration, 1 mM protein (C2A domain/aFGF) was injected in 47 × 6 μL aliquots using the default injection rate. The resulting titration curves were corrected for the protein-free buffer (10 mM sodium phosphate containing 100 mM NaCl) control and analyzed using the Origin ITC software supplied by Micro Cal. Inc. Small unilamellar vesicles of phosphatidyl serine were used to determine the lipid binding affinity of the proteins (aFGF, C2A domain, and aFGF−C2A domain complex). The reaction cell contained the protein. The lipid (phosphatidyl serine) suspensions containing the same buffer were added in serial injections of 6 μL. The concentration of the protein(s) in the cell was about 0.1 mM, whereas the total concentration of the lipids in the syringe was about 20 mM. The binding constants were estimated from the obtained isotherms using the one-site and sequential binding models.

NMR Experiments. All NMR experiments were performed on a Bruker Avance-700 MHz NMR spectrometer equipped with a cryoprobe at 25 °C. ^{15}N decoupling during data acquisition was accomplished using the globally optimized altering phase rectangular pulse sequence, and 2048 complex data points were collected in the ^{15}N dimension. ^{1}H-^{15}N HSQC spectra were recorded at 64 scans at different pH values. The concentration of the protein sample used was 0.1 mM in 90% H_2O and 10% D_2O (10 mM sodium

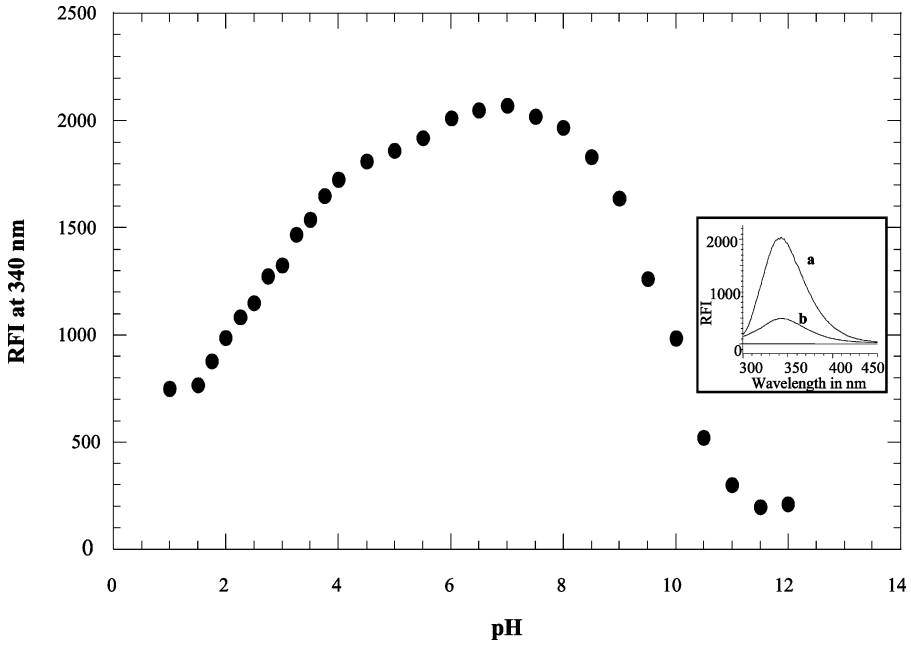

FIGURE 1: pH-induced unfolding profile of the C2A domain monitored by changes in fluorescence at 340 nm. The inset shows the emission spectra of the C2A domain at pH 6.0 (curve a) and pH 3.4 (curve b). The concentration of the C2A domain used was 50 μM. The excitation and emission bandwidths were set to 5 and 10 nm, respectively. The pH of the sample solutions were adjusted manually with a maximum error of $\pm$0.2 units from the desired pH.

phosphate containing 100 mM NaCl). The spectra were processed on a Windows workstation using Xwin-NMR and Sparky software (*52*).

RESULTS

pH Stability of aFGF and the C2A Domain. The stability of aFGF and the C2A domain of p40 Syt1, at various pH, was monitored by changes in intrinsic tryptophan fluorescence. The fluorescence spectrum of aFGF is dominated by tyrosine emission at 308 nm (*3*). The fluorescence of the lone tryptophan at position 121 is quenched by the presence of proximate positive charges in the three-dimensional structure of the protein. This quenching effect is completely relieved in the denatured state(s) of aFGF, and the characteristic tryptophan emission is observed at 350 nm (Supporting Information, Figure S1, inset). Hence, the emission intensity at 350 nm is a reliable probe to monitor the conformational changes induced in aFGF during the pH-dependent unfolding process. pH-induced unfolding curves of aFGF, monitored by changes in the emission intensity at 350 nm, show that the protein is most stable in the pH range between 6.0 and 7.5. The protein begins to unfold on either sides of this pH range. On the alkaline side of pH, complete unfolding of aFGF occurs beyond a pH value of about 9.5 (Supporting Information, Figure S1). On the acidic side, the protein appears to exist in the denatured state at pH values less than 3.0. The decrease in emission intensity (at 350 nm) observed between pH 3.0 and 2.0 can possibly be attributed to the aggregation of the protein (Supporting Information, Figure S1). The pH-induced unfolding profile of the C2A domain, monitored by changes in fluorescence at 340 nm, shows that the protein domain is maximally stable in the pH range between pH 6.0 to 7.5 (Figure 1, inset). The C2A domain unfolds progressively in both the acidic and alkaline range of pH (Figure 1). Complete unfolding of the C2A domain appears to occur at pH values less than 2.0 and greater than 12.0 (Figure 1). The results of the pH-induced unfolding experiments clearly suggest that both aFGF and C2A undergo unfolding under acidic (pH $<$ 5.0) and basic (pH $>$ 8.0) conditions.

Urea-Induced Equilibrium Unfolding of Both aFGF and the C2A Domain under Acidic Conditions (pH $\sim$ *3.4) Is Non-Cooperative.* Urea-induced equilibrium unfolding of aFGF and the C2A domain of Syt1 (at pH 3.4) was monitored by steady-state fluorescence and far-UV circular dichroism (CD) spectroscopy. The urea-induced unfolding profile of aFGF at pH 3.4, monitored by changes in the fluorescence intensity at 350 nm, shows that the protein is denatured completely in urea concentrations greater than 0.5 $\pm$ 0.02 M urea (Supporting Information, Figure S2). The urea-induced unfolding profile of aFGF, obtained under similar experimental conditions by monitoring ellipticity changes (at 228 nm), shows that the protein is completely denatured in 0.4 $\pm$ 0.02 M urea (Supporting Information, Figure S2). The urea-induced unfolding of aFGF, at pH 3.4, is completely reversible. The unfolding curves obtained using CD and fluorescence experiments do not superimpose, suggesting that the urea-induced equilibrium unfolding of aFGF is non-cooperative involving the formation of equilibrium intermediates (Supporting Information, Figure S2). It may be of interest to note that the urea-induced equilibrium folding of aFGF, at pH 6.0, is both reversible and cooperative. The unfolding profiles obtained at pH 6.0, using steady-state fluorescence and far-UV CD spectroscopy, are completely superimposable (*36*).

The urea-induced equilibrium unfolding profile of the C2A domain (at pH 3.4), monitored by changes in intrinsic tryptophan fluorescence at 340 nm, shows that most of the C2A molecules exist in their native state conformation in the urea concentration range of 0 to 0.4 M (Figure 2). The C2A domain begins to unfold in 0.5 M urea, and complete unfolding of the protein domain occurs beyond 1 M urea

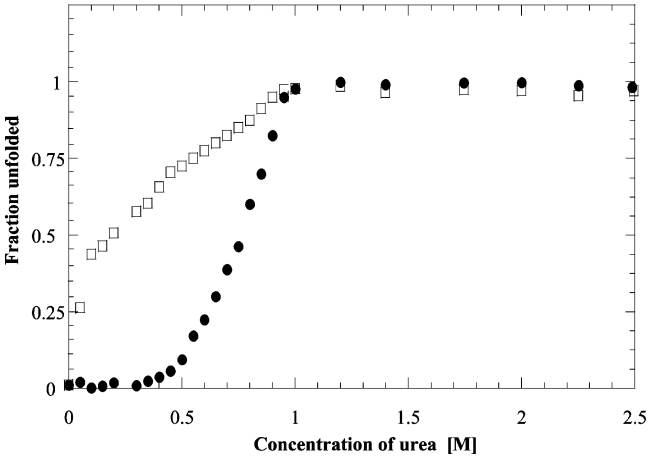

FIGURE 2: Fraction of unfolded species of the C2A domain formed at various concentrations of urea at pH 3.4. The unfolding profile was monitored by the changes in the emission intensity at 340 nm (●) and ellipticity at 218 nm (□). The C_m value for the urea-induced unfolding of the C2A domain estimated from the fluorescence experiments is 0.78 ± 0.05 M.

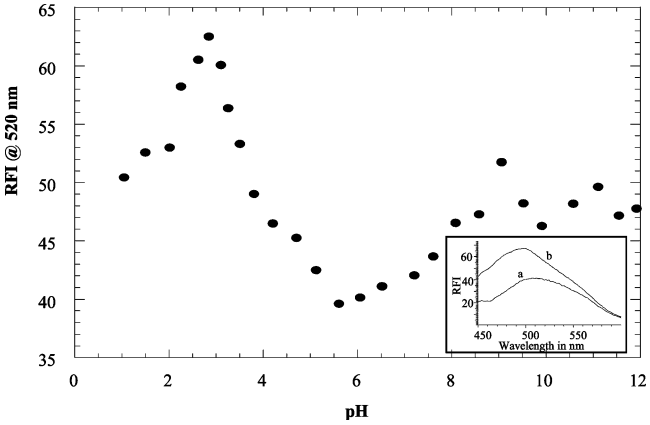

FIGURE 3: ANS binding affinity of the C2A domain at various pH. The inset depicts the emission spectra of the C2A domain at pH 6 (curve a) and pH 3.4 (curve b). The concentration of the protein used was 50 μM. Fluorescence spectra were acquired using an excitation wavelength of 390 nm and an emission wavelength range from 400 to 600 nm. The pH of the solutions were checked repeatedly after the addition of the proteins and ANS to ensure the accuracy of the measured pH (with an error of ±0.2 pH units).

(Figure 2). The C_m (concentration of the denaturant at which approximately 50% of the protein is unfolded) value characterizing the unfolding of the C2A domain is 0.78 ± 0.05 M. Urea-induced equilibrium unfolding of the C2A domain, obtained on the basis of the ellipticity changes at 218 nm, does not superimpose with that obtained using steady-state fluorescence (Figure 2). The absence of the pre-unfolding baseline (in the unfolding curve obtained using ellipticity changes at 218 nm) precludes the accurate estimation of the parameters of unfolding. It should be of interest to note that the urea-induced equilibrium unfolding (at pH 3.4) of intact p40 Syt1, consisting of both the C2A and C2B domains, is also non-cooperative. The urea-induced unfolding profiles of p40 Syt1, monitored by steady-state fluorescence and CD, are non-superimposable (Supporting Information, Figure S3). In summary, the urea-induced equilibrium unfolding data clearly suggest that the unfolding of both aFGF and the C2A domain (at pH 3.4) is non-cooperative and proceeds with the accumulation of stable intermediate state(s).

aFGF and the C2A Domain Exist as Partially Structured States at pH 3.4. We monitored the pH-induced unfolding of aFGF and the C2A domain by examining the affinity of these proteins for binding to the hydrophobic dye 1-anilino-8-napthalene sulfonate (ANS). ANS is a nonpolar fluorescent dye that binds to hydrophobic regions of proteins (*37*). This fluorescent probe has been immensely useful in the identification of partially structured intermediates that accumulate in the unfolding/refolding pathways of proteins (*38*). ANS exhibits strong affinity to bind to solvent-exposed nonpolar surfaces in partially structured states of proteins. Therefore, ANS can be used to identify the partially structured states that possibly populate during the pH-induced unfolding of aFGF and the C2A domain. In the pH range of 6.0−8.0, aFGF exhibits weak affinity to bind to ANS, suggesting that the protein mostly exists in its native state under these conditions (Supporting Information, Figure S4). However, ANS binding, detected by fluorescence at 520 nm, steadily increases with a decrease in pH (below 6.0; Supporting Information, Figure S4). The 520 nm emission intensity of ANS bound to aFGF at pH 3.4 is at least 6-fold higher than that observed at pH 6.0. In addition, the increase in ANS emission intensity at pH 3.4 is accompanied by a significant blue shift from 520 to 490 nm, indicating the presence of nonpolar solvent-accessible surfaces in the protein (Supporting Information, Figure S4). The ANS emission intensity (at 520 nm) shows a small decrease at pH values less than 3.0, possibly because of the complete unfolding of the protein (Supporting Information, Figure S4). The ANS binding affinity of the C2A domain and the intact p40 Syt1 show a trend similar to that observed for aFGF (Figure 3 and Supporting Information, Figure S5). However, the maximum ANS emission intensity upon binding to the C2A domain at pH 3.4 is only about ∼1.5 times as that observed at pH 6.0 (Figure 3). The wavelength of maximum emission of ANS shows a gradual blue shift with the decrease in pH (Figure 3).

The ANS binding affinity for the aFGF−C2A domain complex was examined to further understand if portions of the solvent-exposed nonpolar surfaces, available in the partially unstructured states (at pH 3.4) of these proteins (aFGF and the C2A domain), become inaccessible to the solvent after their interaction. ANS emission intensity (at 520 nm) in the presence of the aFGF−C2A domain complex is significantly lower than the sum of the fluorescence intensity of ANS obtained individually in the presence of aFGF and the C2A domain (Supporting Information, Figure S6). These results suggest that the formation of the aFGF−C2A domain complex is mostly facilitated by the interaction between the solvent-accessible hydrophobic surfaces in the partially unfolded states formed at pH 3.4. The residual ANS binding affinity of the aFGF−C2A domain complex is probably indicative of the availability of additional solvent-accessible nonpolar surfaces, which are not buried in the binding interface of the protein complex (Supporting Information, Figure S6). The aFGF−C2A domain plausibly interacts with the membrane lipids through these solvent-exposed hydrophobic surface(s).

Size-exclusion chromatography (SEC) is a useful technique for obtaining information on the conformational changes that occur during the unfolding of the protein (*39*). SEC is an

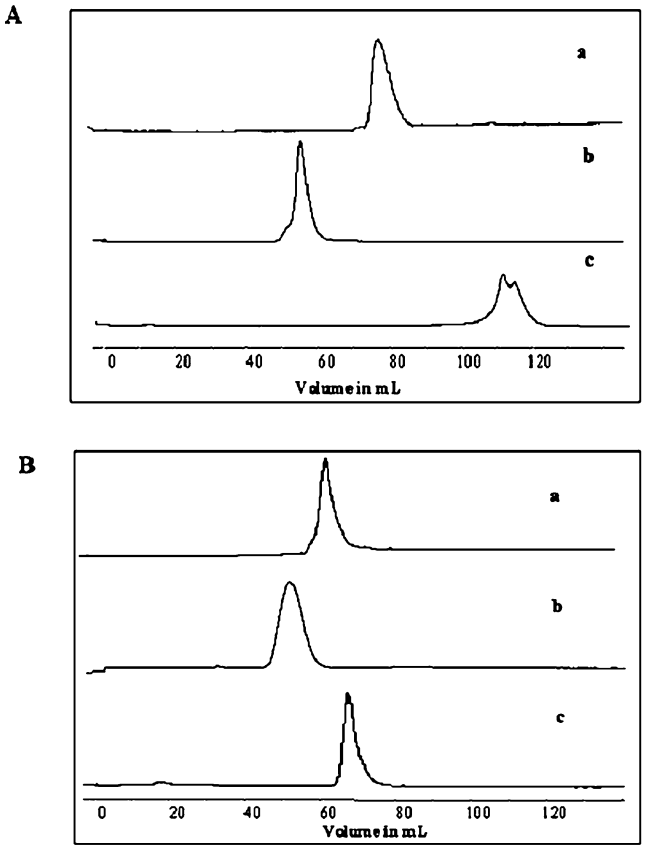

FIGURE 4: (A) Size exclusion chromatography profiles of aFGF (a) at pH 6, (b) denatured state(s) in 8 M urea, and (c) at pH 3.4. (B) Size exclusion chromatography profiles of the C2A domain (a) at pH 6, (b) denatures state(s) in 8 M urea, and (c) at pH 3.4. Elutions of the proteins were monitored by their absorbance at 280 nm. The flow rate of elution was 1 mL/min. The concentration of the proteins used in the experiment was ~100 μM. Elution (25 °C) was carried out using 10 mM phosphate buffer containing 100 mM NaCl.

inert technique that does not perturb the equilibrium between the native, intermediate, and denatured states of proteins (*39*). Therefore, we monitored the relative population of the various molecular states of aFGF and the C2A domain that may exist under various pH conditions. aFGF, in its native state (at pH 6.0), elutes as a single peak with an elution time of 75 ± 0.5 min (Figure 4A-a). aFGF in the denatured state-(s), in 8 M urea, also elutes as a single peak at 52 ± 0.5 min (Figure 4A-b). The SEC elution profile of aFGF at pH 3.4 shows two closely eluting peaks at 108 ± 0.5 and 110 ± 0.4 min. These closely eluted peaks possibly represent the population of molecules in the compact, partially unfolded states (Figure 4A-c). Peaks representing the native (elution time, 75 ± 0.5 min) and denatured states (elution time, 52 ± 0.5 min) of aFGF were completely absent in the elution profile obtained at pH.3.4 (Figure 4A-c). It is surprising to find that the elution times of the peaks representing the partially unfolded states of aFGF (at pH 3.4) are longer than that observed for the denatured states in 8 M urea. It is not reasonable to conceive that the observed longer elution times are due to the highly compact nature of the partially unfolded states of the protein. We believe that longer elution times could be due to the increased affinity of the protein (in its partially structured state at pH 3.4) to the matrix of the size-exclusion column. Such nonspecific interactions between proteins and the inert sepharose resin have been reported previously (*40*).

At pH 6.0, the C2A domain elutes as a single peak with an elution time of 63 ± 0.5 min (Figure 4B-a). The C2A domain in the 8 M urea denatured states also elutes as a single peak at 54 ± 0.5 min (Figure 4B-b). The C2A domain appears to exist as a single population at pH 3.4 because the SEC profile of the protein obtained under these conditions shows a single homogeneous peak (elution time ~68 ± 0.5 min, Figure 4B-c). In summary, the SEC data clearly show that under acidic conditions both aFGF and the C2A domain predominantly exist as partially unfolded states.

Flexibility of the Partially Unfolded States of aFGF and the C2A Domain. Limited proteolytic digestion is an immensely useful technique to probe the gross conformational flexibility of proteins (*41*). In general, proteolytic digestion is governed not only by the stereochemistry and accessibility of the protein substrate but also by the specificity of the proteolytic enzyme. Therefore, subtle conformational changes that occur in a protein during equilibrium unfolding/refolding can be easily monitored by the limited proteolytic digestion technique. Because both aFGF and the C2A domain are rich in arginine and lysine residues, we opted to perform a limited trypsin digestion to probe the conformational flexibility of the proteins in their native state as well as the partially unfolded states that accumulate at pH 3.4. Time-dependent trypsin digestion of the proteins in their native (at pH 6.0) and partially unfolded (at pH 3.4) states was monitored by SDS−PAGE analysis. The percentage of trypsin digestion of aFGF was measured based on the intensity (after Coomoassie blue staining) of the ~17-kDa band (on the polyacrylamide gel) corresponding to the undigested protein (aFGF). The curve depicting the degree of proteolytic cleavage clearly shows that aFGF exists in a partially unfolded state at pH 3.4 (Figure 5A). In the partially unfolded state, the ~17 kDa band representing the intact aFGF molecule completely disappears within 5 min of incubation with trypsin (Figure 5A). It can be argued that the higher cleavage rate of the protein at pH 3.4 is due to activation of the enzyme (trypsin) under given experimental conditions. However, this possibility can be ruled out because control experiments using bovine serum albumin (BSA), at pH 6.0 and pH 3.4, show that the rates of cleavage of BSA by trypsin are nearly same under both pH conditions used (Supporting Information, Figure S7). In marked contrast to BSA, aFGF in its partially structured states (at pH 3.4) is more sensitive to trypsin cleavage than in its native state (at pH 6.0). More than 60% of the protein molecules remain uncleaved even after 40 min of initiation of the cleavage reaction at pH 6.0. These results suggest that large portions of the backbone of aFGF in the partially unfolded state) (observed at pH 3.4) are flexible.

The flexibility of the backbone of the C2A domain in its native (at pH 6.0) and partially unfolded states (at pH 3.4) was compared using the limited trypsin digestion analysis (Figure 5B). The percentage of protection against trypsin cleavage was measured from the intensity of the ~14.8 kDa Coomassie blue stained band (on SDS−PAGE) corresponding to the uncleaved C2A domain. A comparison of the curves depicting the time course of trypsin-induced cleavage of the C2A domain, at pH 6.0 and 3.4, reveals that the protein is more susceptible to cleavage at acidic pH (pH 3.4) than

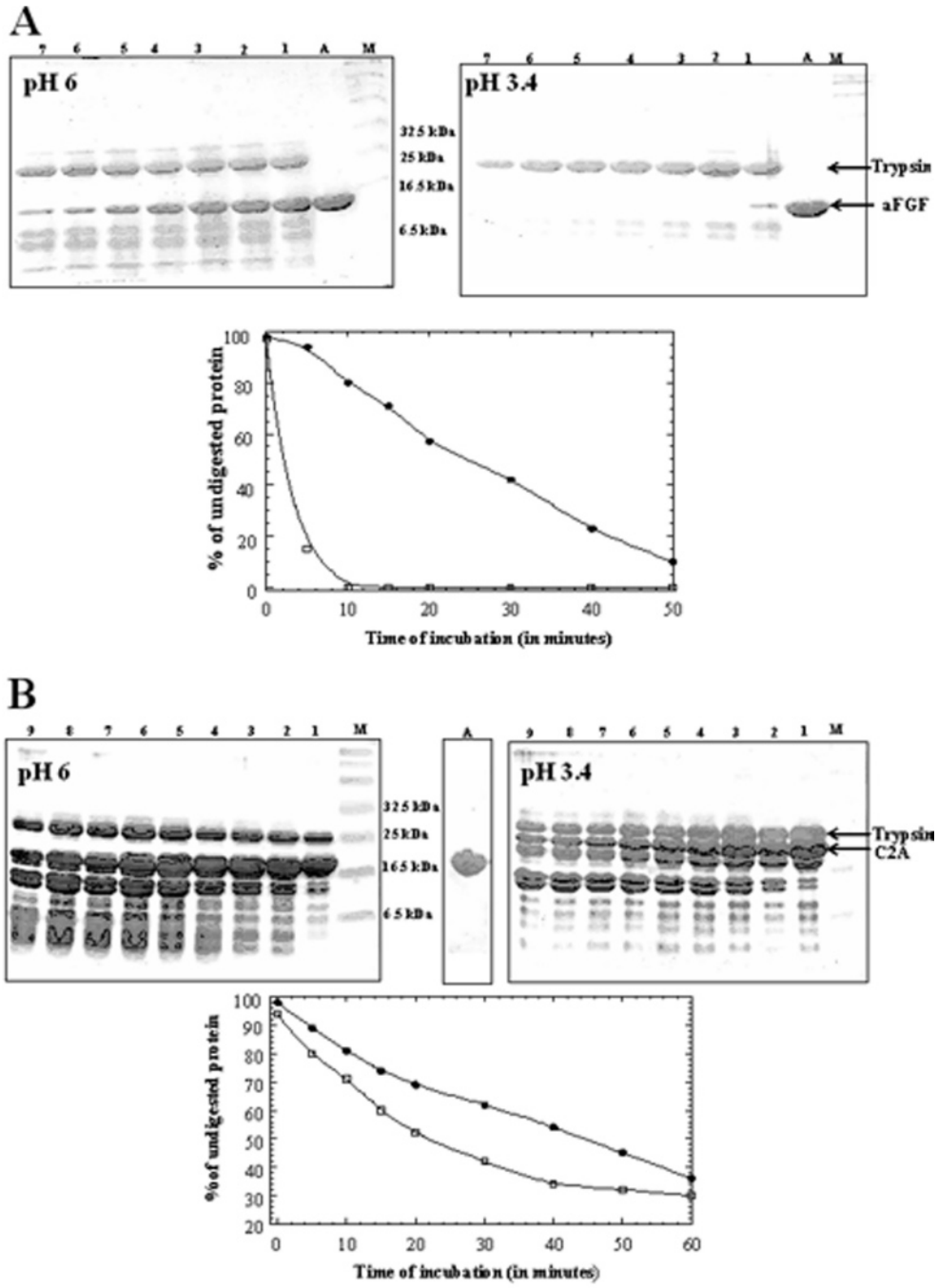

FIGURE 5: (A) SDS−PAGE analysis of the trypsin digestion products of aFGF at pH 6 and pH 3.4 (top panels). The lane marked as A represents the protein band in the absence of trypsin. Lane M shows the molecular weight marker. Lanes, 1−7, represent the trypsin digestion products after various time periods of incubation of aFGF with trypsin at pH 6 and pH 3.4. Lane 1, 5 min; lane 2, 10 min; lane 3, 15 min; lane 4, 20 min; lane 5, 30 min; lane 6, 40 min; and lane 7, 50 min. The ratio of aFGF to trypsin used was 1:1. It is shown that the protein at pH 6.0 was more resistant to trypsin cleavage. The bottom panel depicts the percentage of undigested aFGF at pH 6 (●) and pH 3.4 (○). The percentage of undigested aFGF was estimated from the intensity of the 17 kDa Coomassie blue stained band in the polyacrylamide gel. (B) SDS−PAGE analysis of the trypsin digestion products of the C2A domain at pH 6 and pH 3.4 (top panels). The lane marked as A represents the protein band in the absence of trypsin. Lane M shows the molecular weight marker. Lanes 1−9, represent the trypsin digestion products of the C2A domain at various time periods of incubation of the protein with trypsin at pH 6 and pH 3.4. Lane 1, 5 min; lane 2, 10 min; lane 3, 15 min; lane 4, 20 min; lane 5, 30 min; lane 6, 40 min; lane 7, 50 min; lane 8, 60 min; and lane 9, 70 min. The ratio of the C2A domain to trypsin used was 1:1. The bottom panel depicts the percentage of the undigested C2A domain at pH 6 (●) and at pH 3.4 (○). The percentage of undigested C2A domain was estimated from the intensity of the 14.8 kDa Coomassie blue stained band in the polyacrylamide gel.

at pH 6.0 (Figure 5B). Only 45% of the C2A molecules at pH 6.0 are cleaved after 40 min of initiation of the cleavage reaction. In the partially unfolded state, at pH 3.4, more than 55% of the protein molecules are cleaved after a time span of 40 min (Figure 5B). These results suggest that the partially unfolded intermediate state of the C2A domain is compact and that the flexibility of the backbone of the protein in this state appears to be only marginally higher than that observed in the native state.

Perturbed Regions in the Partially Unfolded States. The ^{1}H-^{15}N HSQC spectrum serves as a fingerprint of the backbone conformation of a protein under given experimental

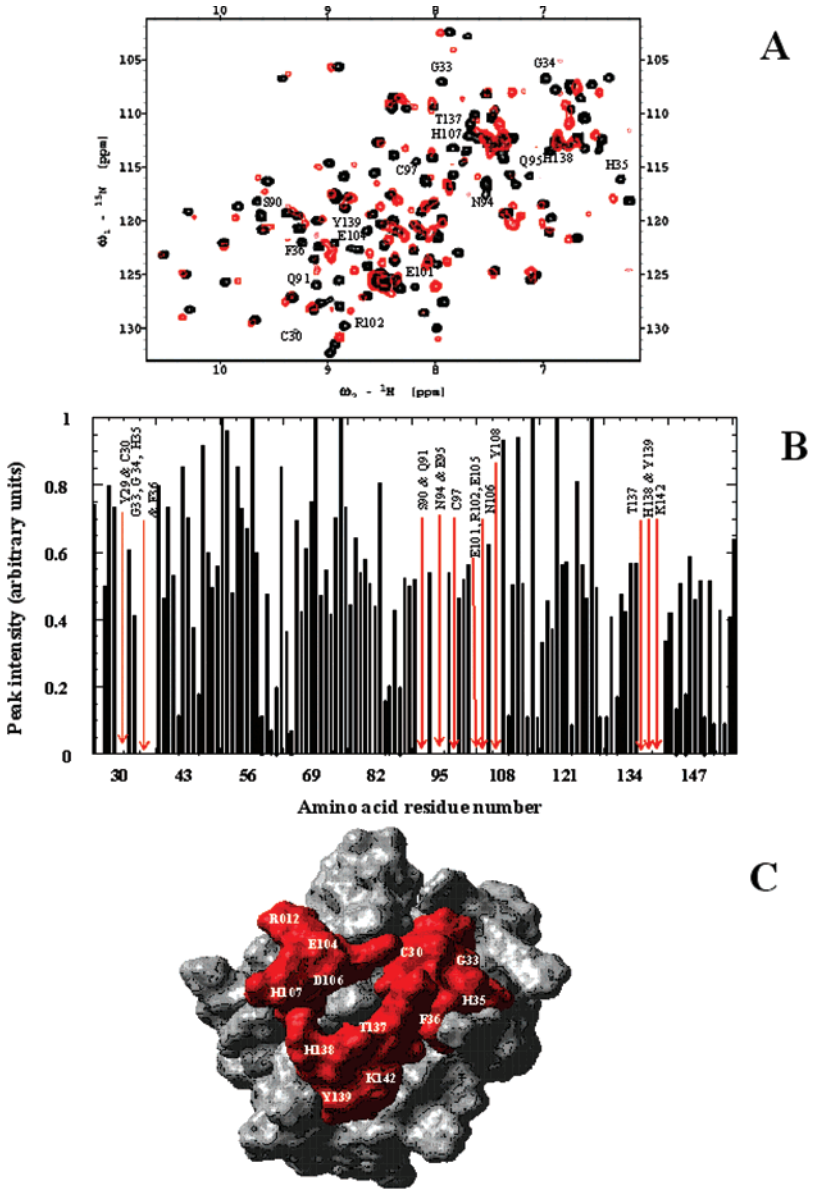

FIGURE 6: (A) Overlap of the ^{1}H-^{15}N HSQC spectra of aFGF at pH 6.0 (black) and pH 3.4 (red). ^{1}H-^{15}N HSQC spectra were obtained at a protein concentration of 100 μM in 10 mM phosphate buffer containing 100 mM NaCl at pH 6 and 3.4 (25 °C). The buffer solutions were prepared in 90% H_2O and 10% D_2O. (B) A plot showing the cross peak intensity of residues in the ^{1}H-^{15}N HSQC spectrum of the aFGF at pH 3.4. Cross peaks that show significant decrease in intensity are shown by red arrows. The cross peaks, which show significant decrease in intensity, represent residues involved in the conformational change. (C) MolMol representation of the structure of aFGF (gray). Residues that show significant decrease in intensity are depicted in red (pH 3.4).

conditions (*42*). ^{1}H-^{15}N HSQC of aFGF in its native state (at pH 6.0) is well-dispersed, indicating that the protein is well-structured (Figure 6A). All the cross-peaks in the HSQC spectrum of aFGF have been previously assigned, and therefore, it is convenient to monitor the structural changes that occur as a function of the pH change. Intensities of selective ^{1}H-^{15}N cross-peaks in the HSQC spectra begin to diminish as the pH is steadily decreased from pH 6.0. At pH 3.4, some of the cross-peaks show drastic chemical shift perturbation, and therefore, they could not be unambiguously traced (Figure 6A). Residues whose cross-peaks disappear in the ^{1}H-^{15}N HSQC spectrum are possibly located in regions of aFGF that become relatively more flexible in the partially unfolded states at pH 3.4. In general, the decrease in cross-peak intensity of selective residues is ascribed to faster internal mobilities of residues in the flexible regions of the protein molecule. Cross-peaks corresponding to Cys30, Gly33, Gly34, His35, Phe36, Ser90, Gln91, Asn94, Glu95, Cys97, Arg102, Glu101, Glu104, His107, Thr137, His138, Tyr139, and Ile144 completely disappeared in the ^{1}H-^{15}N HSQC spectrum of aFGF obtained in pH 3.4 (Figure 6B). These residues are mostly located in β-strand I, β-strand II, β-strand VIII, and the loop connecting β-strands VIII and IX, and β-strand XI (Figure 6C). It appears that many structural interactions stabilizing the native state are largely disrupted in the partially unfolded states of aFGF. The structure of the partially unfolded states of aFGF characterized in this study differs significantly from the one identified by Sanz and Gallego, wherein the acid-induced intermediate state is rigid, retaining most of the native fold of the protein (*32*).

The ^{1}H-^{15}N HSQC spectrum of the C2A domain at pH 6.0 is well-dispersed, indicating that the protein exists in its native state with a well-structured globular fold (Figure 7A).

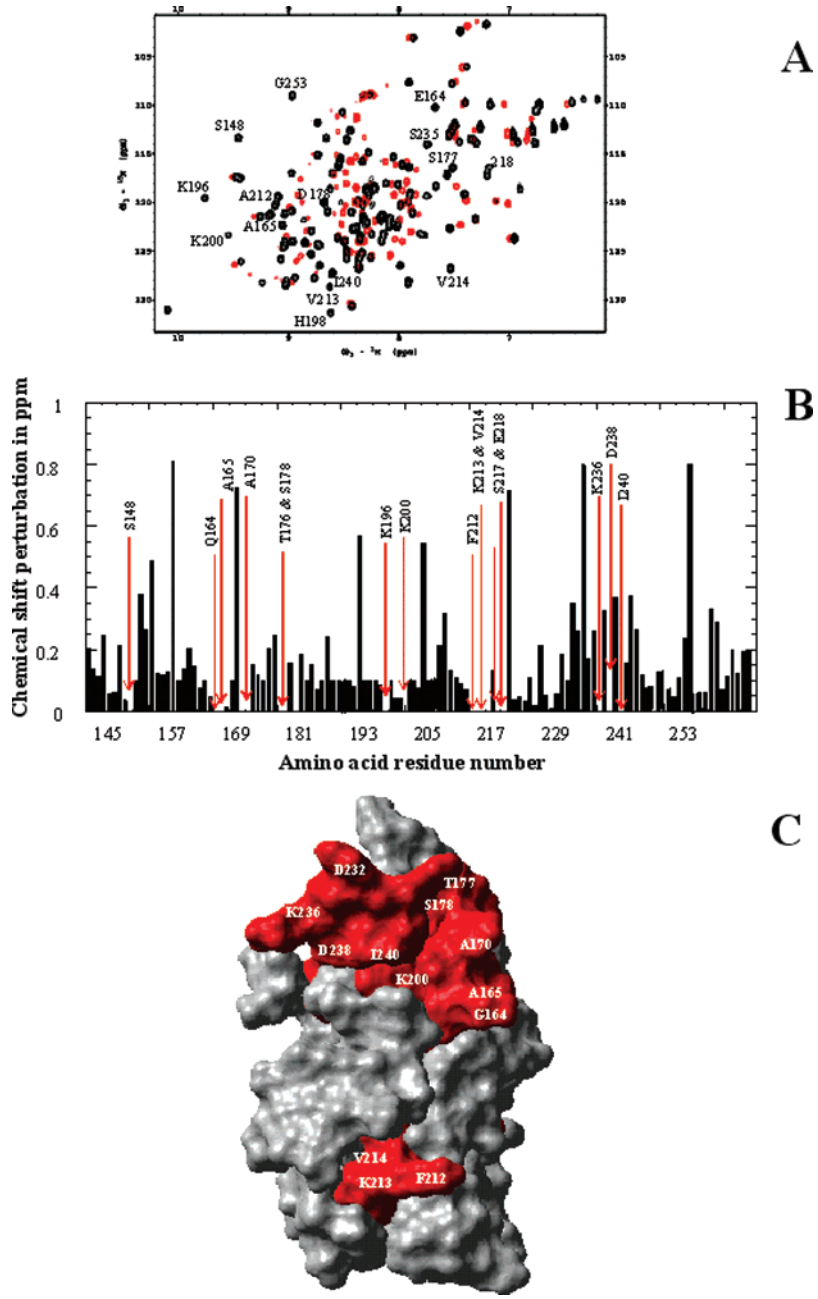

FIGURE 7: (A) Overlap of the ^{1}H-^{15}N HSQC spectra of the C2A domain at pH 6.0 (black) and pH 3.4 (red). ^{1}H-^{15}N HSQC spectra were obtained at a protein concentration of 100 μM in 10 mM phosphate buffer containing 100 mM NaCl at pH 6.0 and 3.4 (25 °C). The buffer solutions were prepared in 90% H_2O and 10% D_2O. (B) Plot showing weighted average (of ^{15}N and ^{1}H) chemical shift perturbation [$\Delta\delta = \sqrt{(\delta H^2 + 0.2(\delta^{15}N)^2}$] of residues in the C2A domain at pH 3.4. Cross peaks that show significant decrease in intensity are shown by red arrows. (C) MolMol representation of the structure of the C2A domain (gray). Residues that exhibit significant decrease in intensity are shown in red (pH 3.4).

As in aFGF, many cross-peaks showed gradual loss in intensity with decrease in pH. Many cross-peaks show significant chemical shift perturbation and also disappear in the ^{1}H-^{15}N HSQC spectrum of the C2A domain acquired at pH 3.4 (Figure 7A). Cross-peaks corresponding to Gln157, Leu168, Lys190, Asn203, Leu219, Arg233, Phe252, and Gly253 show significant ^{1}H-^{15}N chemical shift perturbation (Figure 7B). Cross-peaks of some other residues in the HSQC spectrum also show a dramatic ^{1}H-^{15}N chemical shift perturbation, and therefore, their movement could not be clearly traced. The cross-peaks of residues that disappear in the HSQC spectrum acquired at pH 3.4 include Gln164, Ala165, Ala170, Thr177, Ser178, Lys196, His198, Lys200, Phe212, Lys213, Val214, Glu218, Ser235, and Ile240 (shown by red arrows in Figure 7B). Interestingly, most of these residues are located in the unstructured loop regions connecting the β-strands in the protein (Figure 7C). This observation is consistent with the results of the limited proteolytic digestion experiments, which show that the conformational flexibility of the C2A domain in its native and partially structured states is not significantly different. It appears that most of the native secondary structural interactions are preserved in the partially unfolded states of the C2A domain populated at pH 3.4.

aFGF and C2A Domain Bind Strongly under Acidic Conditions. The binding affinities of aFGF and C2A, at pH

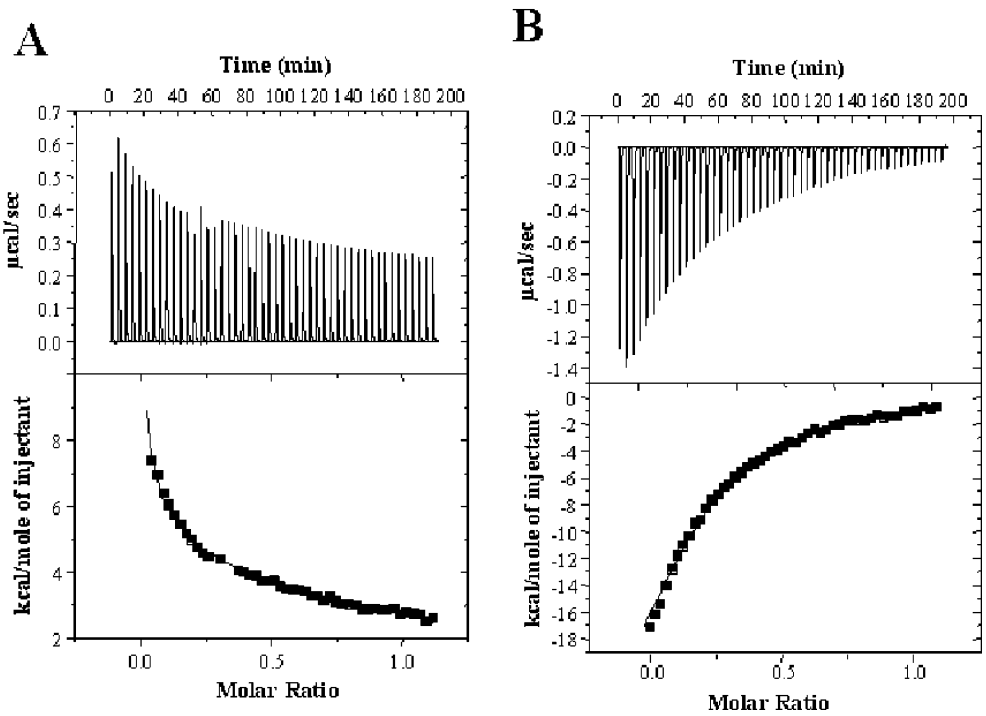

FIGURE 8: (A) Isothermogram depicting the binding of the C2A domain with aFGF at pH 6. The apparent binding constant ($K_{d(app)}$) characterizing the C2A−aFGF interaction was about 36 μM. The top panel shows the raw titration data, and the bottom panel represents the best-fit curve of the raw data. (B) Isothermogram depicting the binding of C2A with aFGF at pH 3.4. The apparent binding constant ($K_{d(app)}$) characterizing the C2A domain−aFGF interaction was about 180 nM. C2A domain and aFGF were observed to bind at a 1:1 stoichiometry. The concentrations of the C2A domain and aFGF used in the ITC experiments are 1 and 0.1 mM, respectively. The top panel shows the raw titration data, and the bottom panel represents the best-fit curve of the raw data.

6.0 and 3.4, were compared using ITC. The binding isotherm representing the interaction between aFGF and the C2A domain at pH 6.0 shows that the interaction between the proteins proceeds with the absorption of heat ($\Delta H \sim 1.3 \pm 0.2$ kcal mol^{-1}). At pH 6.0, aFGF and the C2A domain interact with an apparent binding constant ($K_{d(app)}$) value of about 36 μM (Figure 8A). Interestingly, the best-fit of the titration curve of aFGF versus the C2A domain obtained at pH 3.4 shows that the binding affinity between these interacting proteins increases by 20-fold ($K_{d(app)} \sim 180$ nM, Figure 8B). The binding stoichiometry between aFGF and the C2A domain is estimated to be about 1:1 (under both pH conditions, Figure 8A and B). These results show that acidic conditions strengthen the interaction between aFGF and the C2A domain. The enhanced affinity between the protein constituents under acid conditions is likely to be important in the translocation process of the multiprotein FGF release complex.

Binding of aFGF and the C2A Domain to Phosphatidyl Serine Liposomes Increases under Acidic Conditions. aFGF, which lacks the signal peptide, has to be secreted into the extracellular compartment for it to exhibit its cell proliferation activity by binding to the cell surface receptor (*7*). Maciag and co-workers demonstrated that the secretion of signal peptide-less aFGF occurs through the non-classical route (*15*). aFGF is secreted into the extracellular medium as a multiprotein release complex consisting of aFGF, S100A13, and p40 Syt1 (composed of the C2A and the C2B domains). Prudovsky et al., studying the spatio-temporal aspects of the non-classical export pathway of aFGF employing real-time analysis using confocal microscopy, showed that heat shock stimulates the redistribution of aFGF from a diffuse cytosolic pattern to a locale near the inner surface of the plasma membrane where it co-localized with S100A13 and Syt1 (*22*). Two of the components of the multiprotein release complex, namely, aFGF (*23*) and p40 Syt1, are known to bind to phospholipids. Mutations of specific lysine clusters in these proteins result both in the decrease of liposome permeabilization and blockage of release from the cells (*33*).

It will be interesting to understand if the membrane-binding affinities of aFGF and the C2A domain increase under acidic conditions. In this context, we compared the individual binding affinities of aFGF and the C2A domain to model small unilamellar vesicles (SUVs) of phosphatidyl serine (pS) at pH 6.0 and 3.4. We used model vesicles of pS because in an earlier study, Mach and Middaugh demonstrated the interaction between aFGF with pS under neutral conditions (*28*). aFGF binds to pS vesicles at both pH 6.0 and 3.4 (Figure 9A and B). Interestingly, the apparent binding constant characterizing the interaction between aFGF and pS at pH 3.4 ($K_{d(app)} \sim 478$ nM) is almost three orders of magnitude higher than that observed at pH 6.0 ($K_{d(app)} \sim 384$ μM). Similarly, ITC data show that the C2A domain binds to pS vesicles with higher affinity at pH 3.4 (Figure 9D) than at pH 6.0 (Figure 9C). The apparent binding constant of the C2A−pS interaction at pH 3.4 ($K_{d(app)} \sim 29$ nM) is about 100-fold higher than that observed at pH 6.0 ($K_{d(app)} \sim 270$ μM). Interestingly, the binding isotherm representing the titration of the aFGF−C2A domain complex with SUVs of pS reveals that the protein complex (aFGF−C2A domain complex) also binds to the lipid vesicles but with a lower affinity ($K_{d(app)} \sim 30$ μM) than that of aFGF or the C2A domain alone (Figure 9E). The results of the ITC experiments unambiguously show that both protein−lipid and protein−protein interactions are dramatically strengthened under acidic conditions.

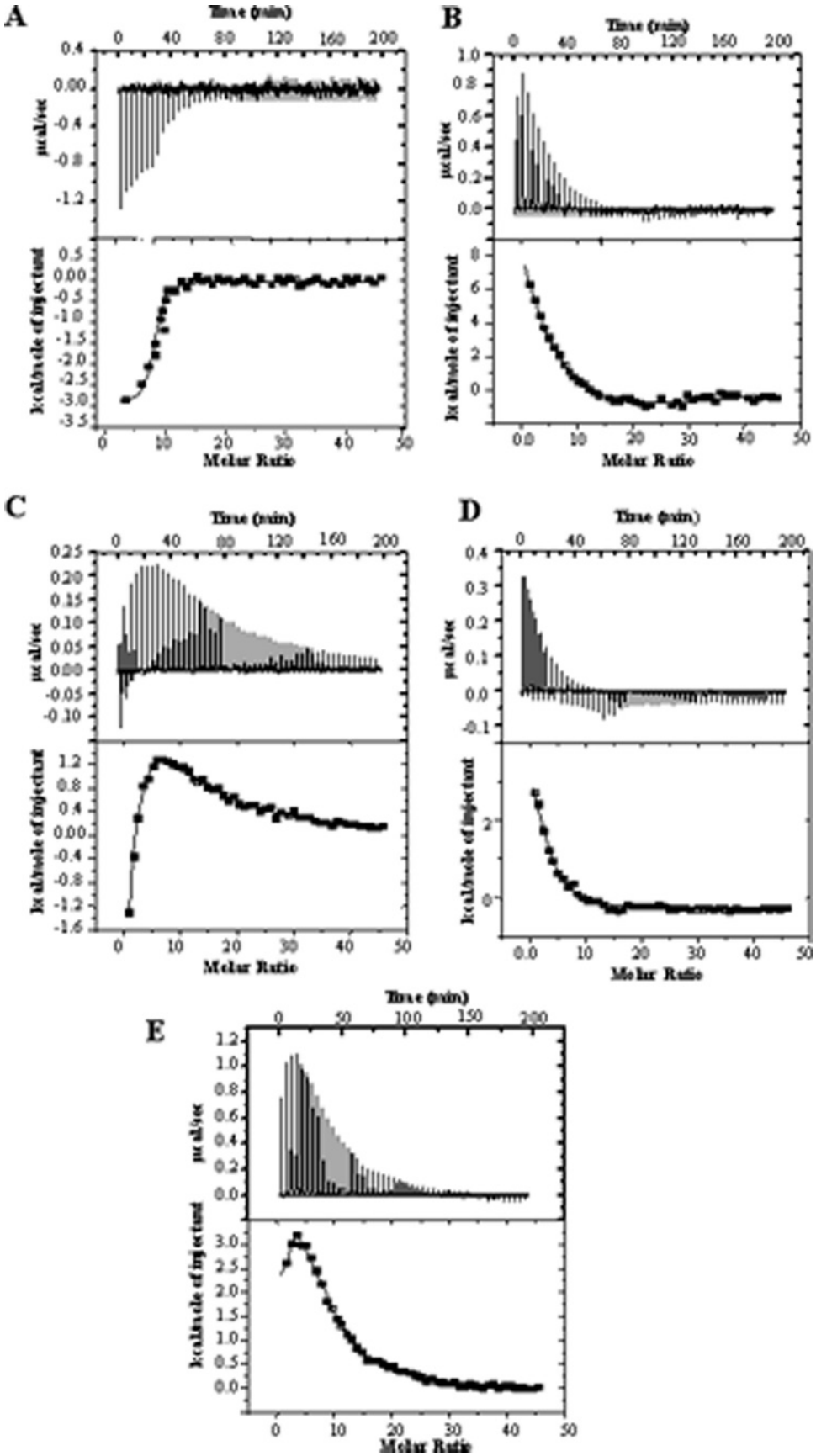

FIGURE 9: ITC curve showing the binding of small unilamellar pS with aFGF at 25 °C, (A) at pH 6 and (B) at pH 3.4. The upper panels show the raw data for the titration of approximately 20 mM lipid vesicles to 0.1 mM protein. The bottom panels show the integrated data obtained from the previous raw data, after subtracting the dilution experiments. The solid line in the bottom panels represents the best-fit curve of the experimental data, using the one site model from Microcal Origin. Isothermograms representing the binding of small unilamellar vesicles of pS with the C2A domain (C) at pH 6 and (D) at pH 3.4. (E) Isothermogram representing the binding of small unilamellar pS with complex of aFGF and the C2A domain at pH 3.4. The solid line in the bottom panels represents the best-fit of the experimental data, using a sequential binding site model from Microcal Origin.

DISCUSSION

Possible Physiological Relevance of the Partially Unfolded States Observed under Acidic Conditions. Our results demonstrate that acidic conditions induce partially structured states of aFGF and the C2A domain of p40 Syt1 and strongly enhance their binding to artificial membranes as well as to each other. We hypothesize that local acidic conditions existing in the vicinity of the cell membrane can be favorable for the non-classical protein release.

Partially unfolded states such as the molten globule states are involved in key cellular processes, such as protein recognition by chaperones (*43*), penetration of proteins across biomembranes (*44*), and release of ligands bound to proteins (*45*). The penetration of certain types of peptide toxins into membranes is known to involve partial unfolding (*25*). This raises an important question as to what causes the protein to unfold at the membrane surface. Elegant studies by Endo and Schatz revealed that the strong negative potential at the membrane surface attracts protons from the bulk solution resulting in a local decrease in pH, which consequently promotes the partial unfolding of proteins (*46*). Studies by Bychkova and Ptitsyn (*47*) and Wilkinson and Mayer (*48*) suggest that the membrane surface has a low dielectric constant. The acidic pH and the low dielectric constant at the membrane surface are shown to produce a denaturing microenvironment at the membrane surface. These studies strongly hint that the partially unfolded states of proteins, such as aFGF and the C2A domain, observed at acidic pH may be physiologically meaningful.

On the basis of the available literature and the results obtained in this study, we are tempted to propose a hypothetical sequence of structural events that possibly occur leading to the translocation of the multiprotein FGF release complex across the cell membrane. As suggested by Prudovsky et al., the first event in the non-classical release pathway appears to be the migration of cytosolic components of the aFGF release complex to the cell membrane (*15*, *22*). This event possibly occurs under the neutral pH conditions prevailing in the cytosol. Subsequently, the multiprotein complex appears to move closer to the inner surface of the membrane (*22*). Upon reaching the membrane surface, the protein constituents of the complex face an acidic microenvironment (due to the strong negative potential and low dielectric constant at the membrane surface), which in turn induces partial unfolding of the proteins (including aFGF and the C2A domain of p40 Syt1). Partial unfolding of the proteins in the multiprotein release complex exposes nonpolar surfaces to the solvent and consequently facilitates interaction with the membrane bilayer. These results clearly suggest that the membrane-binding interface of the multiprotein release complex is possibly provided cooperatively by aFGF and the C2A domain of p40 Syt1. However, in the absence of available data, the participation of S100A13 in membrane binding and membrane translocation cannot be ruled out. The change in free energies of binding of aFGF, the C2A domain, and the aFGF−C2A domain complex (calculated from the ITC data) with pS vesicles show that aFGF possibly translocates individually across the membrane as an unfolded state rather than as a complex with the C2A domain. Once aFGF is released into the extracellular compartment, it is stabilized by the sulfated proteoglycans located on the surface of the cell membrane. Several *in vitro* studies have demonstrated that cellular proteogylcans such as heparin aid in the stabilization of aFGF against pH- and temperature-induced unfolding (*30*). In a recent study, Salamat-Miller et al., using a neural network-based analysis showed that cellular polyanions nonspecifically interact with polyanion-binding proteins such as aFGF and regulate certain cellular events (*49*). The results of several other studies demonstrate that heparin binds to both FGFs and their cell surface receptors (FGFRs) and stabilizes the FGF−FGFR complex. In summary, polysulfated proteoglycans appear to be primarily responsible for the stabilization of aFGF and its interaction with the cell surface receptors. However, the cell surface proteloglycans per se are unlikely to participate in the secretion of aFGF into the extracellular medium.

The molecular mechanism suggested herein may not be far-fetched because cells are known to produce several proteins in their partially structured or unstructured states in high concentrations (*50*). Many important physiological processes, such as exocytosis, endocytosis, and ion-channel activation, are known to involve specific interaction of partially unfolded states of proteins with phospholipids in the cytoplasmic leaflet of the plasma membrane (*51*). At the present stage of knowledge, the mechanism proposed in this study should be considered as hypothetical. More detailed studies aimed at measuring the kinetics of release of aFGF in the presence and absence of the other proteins involved in the multiprotein FGF complex are required to validate the proposed mechanism. Additionally, the effects of mutations interfering with partial protein unfolding at acidic pH upon non-classical release need to be studied.

ACKNOWLEDGMENT

We thank Professor Thomas Sudhof for kindly providing us the C2A and p40 Syt1 clones. We also thank late Professor Tom Maciag for introducing us to research on the non-classical release of FGF. We greatly appreciate the efforts of Norma Albrect in proof reading the manuscript. We would like to thank the anonymous reviewers for their valuable comments on an earlier version of this manuscript.

SUPPORTING INFORMATION AVAILABLE

Figure depicting the stability of aFGF as a function of pH (Figure S1); urea-induced equilibrium unfolding of aFGF monitored by changes in the intrinsic tryptophan fluorescence (Figure S2); urea-induced equilibrium unfolding of intact p40 synaptotagmin-1 monitored by changes in the intrinsic tryptophan fluorescence (Figure S3); ANS binding affinity of aFGF at different pH (Figure S4); ANS binding affinity of intact p40 synaptotagmin 1 at different pH (Figure S5); ANS emission intensity in the presence of the aFGF−C2A domain complex (Figure S6); and SDS−PAGE analysis of the trypsin digestion products of bovine serum albumin (Figure S7). This material is available free of charge via the Internet at http://pubs.acs.org.

REFERENCES

1. Burgess, W. H., and Maciag, R. (1989) The heparin-binding (fibroblast) growth factor family of proteins, *Annu. Rev. Biochem. 58*, 575−606.
2. Arunkumar, A. I., Srisailam, S., Kumar, T. K. S., Kathir, K. M., Chi, Y. H., Wang, H. M., Chang, G. G., Chiu, I., and Yu, C.

(2002) Structure and stability of an acidic fibroblast growth factor from *Notophthalmus viridescens*, *J. Biol. Chem. 277*, 46424−46432.
3. Chi, Y. H., Kumar, T. K. S., Kathir, K. M., Lin, D. H., Zhu, G, Chiu, I. M., and Yu, C. (2002) Investigation of the structural stability of the human acidic fibroblast growth factor by hydrogen-deuterium exchange, *Biochemistry 41*, 15350−15359.
4. Lozano, R. M., Pineda-Lucena, A., Gonzalez, C., Angles, J. M., Cuevas, P., Redondo, H. M., Sanz, J. M., Rico, M., and Gallego, G. (2000). ^{1}H NMR structural characterization of a nonmitogenic, vasodilatory, ischemia-protector and neuromodulatory acidic fibroblast growth factor, *Biochemistry 39*, 4982−4993.
5. Ornitz, D. M. (2005) FGF signaling in the developing endochondral skeleton, *Cytokine Growth Factor Rev. 16*, 205−213.
6. Schlessinger, J., Plotnikov, A. N., Ibrahimi, O. A., Eliseenkova, A. V., Yeh, B. K., Yayon, A., Linhardt, R. J., and Mohammadi, M. (2000) Crystal structure of a ternary FGF-FGFR-heparin complex reveals a dual role for heparin in FGFR binding and dimerization, *Mol. Cell 6*, 743−750.
7. Plotnikov, A. N., Hubbard, S. R., Schlessinger, J., and Mohammadi, M. (2000) Crystal structures of two FGF-FGFR complexes reveal the determinants of ligand-receptor specificity, *Cell 101*, 413−424.
8. Wang, F., McKeehan, K., Yu, C., and Mckeehan, WI. (2002) Fibroblast growth factor receptor 1 phosphotyrosine 766: molecular target for prevention of progression of prostate tumors to malignancy, *Cancer Res. 62*, 1898−1903.
9. Nickel, W. (2005) Unconventional secretory routes: direct protein export across the plasma membrane of mammalian cells, *Traffic (Oxford, U.K.) 6*, 607−614.
10. Backhaus, R., Zehe, C., Wegehingel, S., Kehlenbach, A., Schwappach, B., and Nickel, W. (2004) Unconventional protein secretion: membrane translocation of FGF-2 does not require for folding, *J. Cell Sci. 117*, 1727−1736.
11. Kueltzo, L. A., and Middaugh, C. R. (2003) Nonclassical transport proteins and peptides: an alternative to classical macromolecule delivery systems, *J. Pharm. Sci. 92*, 1754−1772.
12. Mouta Carreira, C., Landriscina, M., Bllum, S., Prudovsky, I., and Maciag, T. (2001) The comparative release of FGF by hypoxia and temperature stress, *Growth Factors 18*, 277−285.
13. Landriscina, M., Bagala, C., Mandinova, A., Soldi, R., Micucci, I., Bellum, S., Prudovsky, I., and Maciag, T. (2001) Copper induces the assembly of a multiprotein aggregate implicated in the release of fibroblast growth factor 1 in response to stress, *J. Biol. Chem. 276*, 25549−25557.
14. Landriscina, M., Soldi, R., Bagala, C., Micucci, I., Bellum, S., Tarantini, F., Prudovsky, I., and Maciag, T. (2001) S100A13 participates in the release of fibroblast growth factor 1 in response to heat shock *in vitro*, *J. Biol. Chem. 276*, 22544−22552.
15. Prudovsky, I., Mandinova, A., Soldi, R., Bagala, R., Graziani, I., Landriscina, M., Tarantini, F., Duarte, M., Bellum, S., Doherty, H., and Maciag, T. (2003) The non-classical export routes: FGF1 and IL-1alpha point the way, *J. Cell Sci. 116*, 4871−4881
16. Ridinger, K., Schafer, B. W., Durussel, I., Cox, J. A., and Heizmann, C. W. (2000) S100A13. Biochemical characterization and subcellular localization in different cell lines, *J. Biol. Chem. 275*, 8686−8694.
17. Sivaraja, V., Kumar, T. K., Prudovsky, I., and Yu, C. (2005) Resonance assignments for mouse S100A13, *J. Biomol. NMR 32*, 257−257.
18. Arnesano, F., Banci, L., Bertini, I., Fantoni, A., Tenori, L., and Viezzoli, M. S. (2005) Structural interplay between calcium(II) and copper(II) binding to S100A13 protein, *Angew. Chem., Int. Ed. 44*, 6341−6344.
19. Shin, O. H., Rizo, J., and Sudhof, T. C. (2002) Synaptotagmin function in dense core vesicle exocytosis studied in cracked PC12 cells, *Nat. Neurosci. 5*, 649−656.
20. Shao, X., Fernandez, I., Sudhof, T. C., and Rizo, J. (1998) Solution structures of the Ca^{2+}-free and Ca^{2+}-bound C2A domain of synaptotagmin I: does Ca^{2+} induce a conformational change? *Biochemistry 37*, 16106−16115.
21. Bai, J., and Chapman, E. R. (2004) The C2 domains of synaptotagmin−partners in exocytosis, *Trends Biochem. Sci. 3*, 143−151.
22. Prudovsky, I., Bagala, C., Tarantini, F., Mandinova, A., Soldi, R., Bellum, S., and Maciag, T. (2002) The intracellular translocation of the components of the fibroblast growth factor 1 release complex precedes their assembly prior to export, *J. Cell. Biol. 158*, 201−208.
23. Tarantini, F., Gamble, S., Jackson, A., and Maciag T. (1995) The cysteine residue responsible for the release of fibroblast growth factor-1 residues in a domain independent of the domain for phosphatidylserine binding, *J. Biol. Chem. 270*, 29039−29042.
24. Lavallee, T. M., Prudovsky, I., McMahon G. A., Hu, X., and Maciag, T. (1998) Activation of the MAP kinase pathway by FGF-1 correlates with cell proliferation induction while activation of the Src pathway correlates with migration, *J. Cell. Biol. 141*, 1647−1658.
25. Wiedlocha, A., Madshus, I. H., Mach, H., Middaugh, C. R., and Olsnes, S. (1992) Tight folding of acidic fibroblast growth factor prevents its translocation to the cytosol with diphtheria toxin as vector, *EMBO J. 11*, 4835−4842.
26. Wesche, J., Wiedlocha, A., Falnes, P. O., Choe, S., and Olsnes, S. (2000) Externally added FGF mutants do not require extensive unfolding for transport to the cytosol and the nucleus in NIH/3T3 cells, *Biochemistry 39*, 15091−15100.
27. Mach, H., Ryan, J. A., Burke, C. J., Volkin, D. B., and Middaugh, C. R. (1993) Partially structured self-associating states of acidic fibroblast growth factor, *Biochemistry 32*, 7703−7711.
28. Mach, H., and Middaugh, C. R. (1995) Interaction of partially structured states of acidic fibroblast growth factor with phospholipid membranes, *Biochemistry 34*, 9913−9920.
29. Burke, C. J., Volkin, D. B., Mach, H., and Middaugh, C. R. (1993) Effect of polyanions on the unfolding of acidic fibroblast growth factor, *Biochemistry 32*, 6419−6426.
30. Edwards, K. L., Kueltzo, L. A., Fisher, M. T., and Middaugh, C. R. (2001) Complex effects of molecular chaperones on the aggregation and refolding of fibroblast growth factor-1, *Arch. Biochem. Biophys. 393*, 14−21.
31. Fan, H., Zhang, M., and Middaugh, C. R. (2007) Effects of solutes on empirical phase diagrams of human fibroblast growth factor 1, *J. Pharm. Sci. 96*, 1490−1503.
32. Sanz, J. M., and Gallego, G. (1997) A partly folded state of acidic fibroblast growth factor at low pH, *Eur. J. Biochem. 246*, 328−335.
33. Graziani, I., Bagala, C., Duarte, M., Soldi, R., Kolev, V., Tarantini, F., Kumar, T. K., Doyle, A., Neivandt, D., Yu, C., Maciag, T., and Prudovsky, I. (2006) Release of FGF1 and p40 synaptotagmin 1 correlates with their membrane destabilizing ability, *Biochem. Biophys. Res. Commun. 349*, 192−199.
34. Bychkova, V. S., Dujsekina, A. E., Klenin, S. I., Tiktopulo, E. I., Uverksy, V. N., and Ptitsyn, O. B. (1996) Molten globule-like state of cytochrome c under conditions simulating those near the membrane surface, *Biochemistry 35*, 6058−6063.
35. de Marco-Lousa, C., Sideris, D. P., and Tokatlids, K. (2006) Translocation of mitochondrial inner-membrane proteins: conformation matters, *Trends Biochem. Sci. 31*, 259−267.
36. Srimathi, T., Kumar, T. K. S., Kathir, K. M., Chi, Y. H., Srisailam, S., Lin, W. Y., Chiu, I. M., and Yu, C. (2003) Structurally homologous all beta-barrel proteins adopt different mechanisms of folding, *Biophys. J. 85*, 459−472.
37. Uversky, V. N., Winter, S., and Lober, G. (1998) Self-association of 8-anilino-1-naphthalene-sulfonate molecules: spectroscopic characterization and application to the investigation of protein folding, *Biochim. Biophys. Acta 1388*, 133−142.
38. Uversky, V. N., Winter, S., and Lober, G. (1996) Use of fluorescence decay times of 8-ANS-protein complexes to study the conformational transitions in proteins which unfold through the molten globule state, *Biophys. Chem. 60*, 79−88.
39. Uversky, V. N. (1993) Use of fast protein size-exclusion liquid chromatography to study the unfolding of proteins which denature through the molten globule, *Biochemistry 32*, 13288−13298.
40. Hajra, S., and Chattoraj, D. K. (1991) Protein adsorption at solid-liquid interfaces: effects of different solid-liquid systems and various neutral salts, *Indian. J. Biochem. Biophys. 28*, 267−279.
41. Wang, L., and Kallenbach, N. R. (1998) Proteolysis as a measure of the free energy difference between cytochrome c and its derivatives, *Protein Sci. 7*, 2360−2464.
42. Schulman, B. A., Kim, P. S., Dobson, C. M., and Redfield, C. (1997) A residue-specific NMR view of the non-cooperative unfolding of a molten globule, *Nat. Struct. Biol. 6*, 630−634.
43. Van der Vies, S. M., Viitanen, P. V., Gatenby, A. A., Lorimer, G. H., and Jaenicke, R. (1992) Conformational states of ribulose-bisphosphate carboxylase and their interaction with chaperonin 60, *Biochemistry 31*, 3635−3644.
44. Van der Goot, F. G., Lakey, J. H., and Pattus, F. (1992) The molten globule intermediate for protein insertion or translocation through membranes, *Trends Cell. Biol. 2*, 343−348.

45. Bychkova, V. E., Bartoshevich, S. F., and Klenin, S. I. (1990) Comparative study of diffusion coefficients of alpha-lactalbumins and lysozyme using polarization interferometer, *Biofizika (Moscow) 35*, 242−248.

46. Endo, T., and Schatz, G. (1988) Latent membrane perturbation activity of a mitochondrial precursor protein is exposed by unfolding, *EMBO J. 7*, 1153−1158.

47. Bychkova, V. E., and Ptitsyn, O. B. (1995) Folding intermediates are involved in genetic diseases? *FEBS Lett. 359*, 6−8.

48. Wilkinson, K. D., and Mayer, A. N. (1986) Alcohol-induced conformational changes of ubiquitin, *Arch. Biochem. Biophys. 250*, 390−399.

49. Salamat- Miller, N., Fang, J., Seidel, C. W., Assenov, Y., Albrecht, M., and Middaugh, C. R. (2007) A network-based analysis of polyanion-binding proteins utilizing human protein arrays, *J. Biol. Chem. 282*, 10153−10163.

50. Dyson, H. J., and Wright, P. E. (2005) Intrinsically unstructured proteins and their functions, *Nat. Rev. Mol. Cell Biol. 6*, 197−208.

51. McLauglin, S., and Murry, S. (2005) Plasma membrane phosphoinositide organization of protein molecules, *Nature 438*, 605−611.

52. Goddard, T. D., and Kneller, D. G. (2006) *SPARKY 3*, University of California, San Francisco, CA.

BI7002586